

Fast and Efficient Removal of Hexavalent Chromium from Water by Iron Oxide Particles

Duangta Kitkaew^{1,2}, Athit Phetrak^{*3}, Sumate Ampawong⁴, Rachaneekorn Mingkhwan³, DOUNGKAMON PHIHUSUT⁵, Kamolnetr Okanurak³ and Chongrak Polprasert⁶

¹Department of Sanitary Engineering, Faculty of Public Health, Mahidol University, Bangkok 10400, Thailand

²Center of Excellence on Environmental Health and Toxicology (EHT), Mahidol University, Bangkok 73170, Thailand

³Department of Social and Environmental Medicine, Faculty of Tropical Medicine, Mahidol University, Bangkok 10400, Thailand

⁴Department of Tropical Pathology, Faculty of Tropical Medicine, Mahidol University, Bangkok 10400, Thailand

⁵Environmental Research Institute, Chulalongkorn University, Bangkok 10330, Thailand

⁶Department of Civil Engineering, Faculty of Engineering, Thammasat University, Bangkok 12120, Thailand

ARTICLE INFO

Received: 25 Sep 2017
 Received in revised:
 21 Nov 2017
 Accepted: 4 Dec 2017
 Published online:
 22 Dec 2017
 DOI: 10.14456/enrj.2018.9

Keywords:

Hexavalent chromium/ Iron oxide particles/ Adsorption/ Pseudo-second order model

* Corresponding author:

E-mail:
 athit.phetrak@gmail.com
 athit.phe@mahidol.ac.th

ABSTRACT

Iron oxide particles (IOPs) were synthesized by chemical co-precipitation technique and further used as an adsorbent in removing hexavalent chromium (Cr(VI)) from aqueous solutions during batch adsorption. The IOP adsorbent had specific surface area of 65 m²/g, total pore volume of 0.25 cm³/g and mostly contained a mesoporous structure. The analysis of scanning and transmission electron microscopy indicated that the adsorbent contained a substantial amount of iron oxide of about 66%, which was well distributed throughout the adsorbent. The IOP adsorbent showed a rapid and efficient Cr(VI) removal that followed Langmuir adsorption isotherm model with maximum adsorption capacity of 2.39 mg-Cr(VI)/g-IOP, demonstrating a monolayer formation on the adsorptive sites of IOP. The kinetic adsorption of Cr(VI) on the IOP followed the pseudo-second-order model, suggesting chemisorption. Thus, the IOP adsorbent provides a potentially effective technology in eliminating of Cr(VI) from water since it can remove appreciable amounts of Cr(VI) with a relatively short contact time of 30 min.

1. INTRODUCTION

Chromium (Cr) is a highly toxic chemical that can cause serious environmental pollution via adverse effects upon living organisms (Lai et al., 2008). It is possibly released from many industries, such as electroplating, mining and leather tanning amongst others to the aquatic environment (Suksabye et al., 2008; Gupta et al., 2011; Kongsricharoern and Polprasert, 1995). Typically, chromium is mainly present as an oxyanion species, which exists as the hexavalent chromium (Cr(VI)) and trivalent chromium (Cr(III)) states, depending on the pH. Among these species, Cr(VI) has the most harmful effects on living organisms, being highly mobile in the environment (Fang et al., 2011). The maximum contaminant level (MCL) for Cr(VI) at 50 µg/L in drinking water is regulated by the World Health Organization, while the United States Environmental Protection Agency regulates a MCL for total Cr at

100 µg/L. The maximum allowed concentration of Cr(VI) and Cr(III) in industrial wastewater effluent in Thailand is 0.25 mg/L and 0.75 mg/L, respectively. Thus, it is necessary to eliminate Cr before discharging into natural water resources.

There are several techniques that have been employed in removing Cr(VI) from solutions, namely adsorption (Suksabye et al., 2008), electrochemical precipitation (Kongsricharoern and Polprasert, 1995), ion exchange resins (Rengaraj et al., 2001), and membrane filtration (Benito and Ruiz, 2002). Among these, adsorption has received the greater interest because of its easy handling, low cost, flexible approach and high removal efficiency (Abussaud et al., 2013). Since it has been found to be efficient at removing Cr(VI) from water samples, one of the most commonly used adsorbents is activated carbon (AC) (Gupta et al., 2011; Chaudhuri and Azizan, 2012; Zou et al., 2015).

However, it is difficult to separate the AC adsorbent from the water by traditional filtration methods (Faulconer et al., 2012). Therefore, development of novel adsorbents with high adsorption and recovery abilities remains as one of the challenges in adsorption research. During the last few decades, iron oxide particles (IOPs) have attracted increasing research attention in the field of environmental remediation (Gupta et al., 2011; Ha et al., 2004; Uwamariya et al., 2015), which is largely due to their advantages in application of being efficient at pollutant removal and being rapidly separated from the solution by installing a magnetic separator.

From the need to explore more suitable adsorbents which have high removal efficiencies and are easy to recover, in this study IOPs were synthesized using simple chemical co-precipitation and then used as an adsorbent for Cr(VI) adsorption in aqueous solutions. The morphology of the obtained IOP adsorbent was viewed by scanning electron microscopy (SEM) coupled with energy dispersive spectrometer (SEM-EDS). Meanwhile, the analysis of transmission electron microscopy (TEM) as well as Brunauer-Emmett-Teller (BET) surface area were also conducted. Batch experiments of isotherm and adsorption kinetics were performed to determine the adsorptive behavior of Cr(VI) and its removal mechanism on the IOP adsorbent.

2. METHODOLOGY

2.1 Preparation of IOPs as an adsorbent

The IOP adsorbent was prepared by chemical co-precipitation, adapted from the method of Han et al. (2015). Briefly, 18.3 g of $\text{FeSO}_4 \cdot 7\text{H}_2\text{O}$, 33.3 g of $\text{FeCl}_3 \cdot 6\text{H}_2\text{O}$ and 1,000 mL of Milli-Q water were combined in a 2,000-mL beaker and mixed by magnetic stirrer. After complete dissolution, the solution was gradually heated to 65 °C and then cooled down using ice water to below 40 °C before 5 N NaOH was added drop wise under vigorous stirring to increase the pH solution to 10-11. The resulting suspension was stirred constantly for 1 h and then left overnight to precipitate. The supernatant was discarded and the precipitated IOP was rinsed twice with 1,000 mL of Milli-Q water and twice with ethanol. Subsequently, the IOP suspension was transferred into 50-mL conical centrifuge tubes and then centrifuged for 3-5 min at 3,000 rpm. Thereafter, the IOP pellets were harvested, dried in an oven at 70-75 °C for 48 h and

then manually ground and sieved to obtain a 20-50 mesh fraction which was kept in an air-tight container until further use.

2.2 Characterization of the IOPs

The surface morphology of the IOP adsorbent, including specific surface area, total pore volume and pore size distribution, was measured using the surface area analyzer (Quantachrome, Autosorb-1). Before measurement, the adsorbent was dried and degassed. The BET specific surface area of IOP adsorbent was calculated using the linear plot of BET adsorption. The total pore volume and average pore diameter of the IOP adsorbent were determined by nitrogen (N_2) gas adsorption and desorption at 77 K with the surface area analyzer (Quantachrome, Autosorb-1). The surface properties and elemental compositions of the IOP adsorbent were characterized using TEM (Hitachi-HT7700) and SEM-EDS (Hitachi-SU3500, Japan).

2.3 Chromium adsorption onto IOPs

All adsorption experiments were conducted using a bottle point method. In this work, a Cr(VI) stock solution of 1000 mg/L was prepared using analytical grade of potassium dichromate ($\text{K}_2\text{Cr}_2\text{O}_7$) and thereafter diluted to the desired concentration with Milli-Q water. Small volumes of NaOH and HCl were used to adjust the pH to 6.5 ± 0.2 . Batch adsorption experiment was conducted by adding the desired amount of IOP adsorbent into a 100-mL flask containing Cr(VI) solution of 50 mL of and then shaken at 220 rpm at 25 °C for the specified period of time, after which the IOP was separated from the water by filtration through a pre-rinsed 0.45- μm nylon filter. Analysis of concentration of Cr(VI) in aqueous solution was performed using 1,5 diphenylcarbazide at 540 nm by spectrophotometer (U-2700, Shimadzu). Each experiment was carried out in replicate samples under the same conditions. Meanwhile, the average value was reported with the standard deviation (SD) as error bars. The adsorbed Cr(VI) and its removal by IOP were calculated as shown in Equations (1) and (2), respectively:

$$q_e = \frac{(C_i - C_e)}{m} \times V \quad (1)$$

$$\text{Removal efficiency of CR(VI)(\%)} = \frac{(C_i - C_e)}{C_i} \times 100 \quad (2)$$

where q_e represents the amounts of Cr(VI) adsorbed on IOPs (mg/g), C_i and C_e represent initial and equilibrium Cr(VI) concentration in solution phase (mg/L), respectively. V is the solution volume of Cr(VI) (L) used in the experiments, while m represents the weight of IOPs (g).

2.4 Adsorption isotherm

Adsorption isotherm models were employed to analyze the adsorptive behavior of Cr(VI) on the IOPs. In this work, the equilibrium adsorption data of Cr(VI) at various IOP dosages were fitted by the empirical Langmuir and Freundlich adsorption isotherm models. The linear form of the Langmuir isotherm model is displayed in Equation (3) (Langmuir, 1918):

$$\frac{C_e}{q_e} = \frac{1}{q_{max}b} + \frac{C_e}{q_{max}} \quad (3)$$

where q_{max} represents the maximum adsorption capacity for Cr(VI) on IOPs (mg/g), while b is the constant of Langmuir isotherm related to the apparent energy of adsorption. Then Langmuir isotherm constants (q_{max} and b) can be calculated from the slope and intercept of a plot between C_e/q_e and C_e . The separation factor or dimensionless constant (R_L) can be determined from Langmuir adsorption isotherm as shown in Equation (4):

$$R_L = \frac{1}{1 + C_i b} \quad (4)$$

The characteristics of Langmuir adsorption isotherm are explained by the average value of R_L . The tendency of adsorption system can be associated to irreversible adsorption, when the value of R_L is equal to 0. The value of R_L between 0 and 1 ($0 < R_L < 1$) is indicated as favorable adsorption. The adsorption system is linear adsorption, when the value of R_L is equal to 1. The unfavorable adsorption is present, the value of R_L is greater than 1. The Freundlich isotherm model is expressed in Equation (5) (Freundlich, 1906):

$$\log q_e = \log K_f + \frac{1}{n} (\log C_e) \quad (5)$$

where K_f represents the adsorptive capacity of Freundlich isotherm model (mg/g). The n can be indicated the favorability of adsorption. Both K_f and

n values can be obtained from the intercept and slope of a plot of $\log q_e$ versus $\log C_e$, respectively.

2.5 Adsorption kinetics

To investigate the mechanism of Cr(VI) removal by IOP from aqueous solution, adsorption kinetic experiments were conducted. Two kinetic models of Lagergren pseudo-first order (Lagergren, 1898) and the pseudo-second order model (Ho et al., 2000) were utilized to analyze the kinetic adsorption data, as shown in Equations (6) and (7), respectively:

$$\log(q_e - q_t) = \log q_e - \frac{k_1 t}{2.303} \quad (6)$$

$$\frac{t}{q_t} = \frac{1}{k_2 q_e^2} + \frac{t}{q_e} \quad (7)$$

where q_e represents the equilibrium amounts of Cr(VI) adsorbed on IOP (mg/g), while q_t is amounts of Cr(VI) adsorbed on IOP (mg/g) at time t (min). The k_1 value represents the rate constant of the pseudo-first-order (1/min), while k_2 value indicates the rate constant of the pseudo-second-order adsorption (g/mg·min).

3. RESULTS AND DISCUSSION

3.1 The properties of the IOP adsorbent

The surface structure of the IOPs was observed using SEM (Figure 1(a) and (b)), where the aggregated surface structure of the IOPs was evident at a low magnification ($\times 12,000$), but at a higher magnification ($\times 30,000$) a spongy-like structure covering the aggregated IOPs was evident. In order to affirm the coverage of the iron oxide on the IOP adsorbent, EDS was applied and revealed that the elemental composition of the IOP adsorbent included 66% iron, 29% oxygen and 5% carbon. This indicated that the surface structure of the IOP adsorbent was densely covered by iron oxides.

To support the SEM observation, TEM was used to visualize the distribution and shape of the IOPs. Iron particles were distributed uniformly on single adsorbent particles as seen in Figure 2, while an aggregation of iron particles was found on the flocculated adsorbent, which may have occurred during formation (Hu et al., 2005; Hu et al., 2004). It was clearly seen that the IOPs were spherical, but the size of the IOPs were diverse, which could be influenced by the growth time and substrate concentration (Lu et al., 2002).

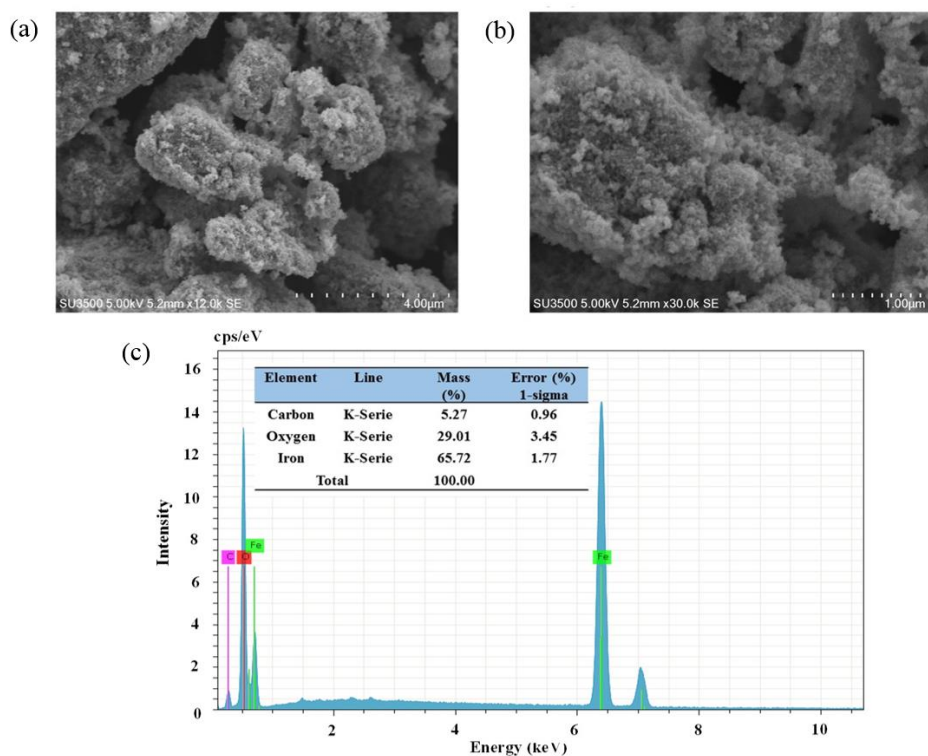


Figure 1. SEM images at (a) $\times 12,000$ and (b) $\times 30,000$ magnification and (c) the elemental composition of the IOP adsorbent.

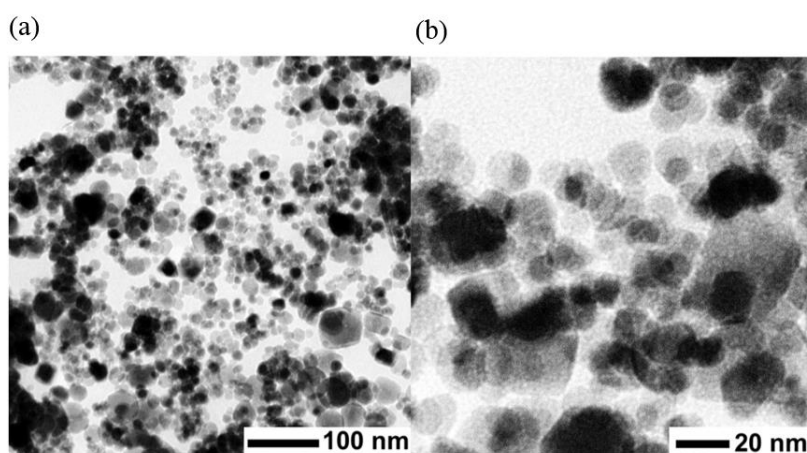


Figure 2. TEM images of the (a) distribution of IOPs on the adsorbent particles ($\times 40,000$ magnification) and (b) association of IOPs with adsorbent particles ($\times 150,000$ magnification).

As shown in Figure 3, the N_2 adsorption-desorption isotherms exhibited a IV-type curve of a hysteresis loop, according to IUPAC classification, consistent with the typical characteristics of a mesoporous material (Sing, 1982; Deng et al., 2008; Lei et al., 2014). The average pore diameter was 15.48 nm, which falls within the range of a mesoporous structure (2-50 nm), while the total pore volume was $0.2532 \text{ cm}^3/\text{g}$. The specific surface area,

one of the most important properties that influence the kinetic reaction, was calculated to be $65.42 \text{ m}^2/\text{g}$, Figure 3 (inset table), which is similar to the specific surface area of pure iron oxide ($66 \text{ m}^2/\text{g}$) (Oliveira et al., 2002), but higher than that for nanoscale zero-valent iron ($35 \text{ m}^2/\text{g}$) (Fang et al., 2011). With respect to these results, the IOP adsorbent was attractive for contaminant elimination because of its high specific surface area.

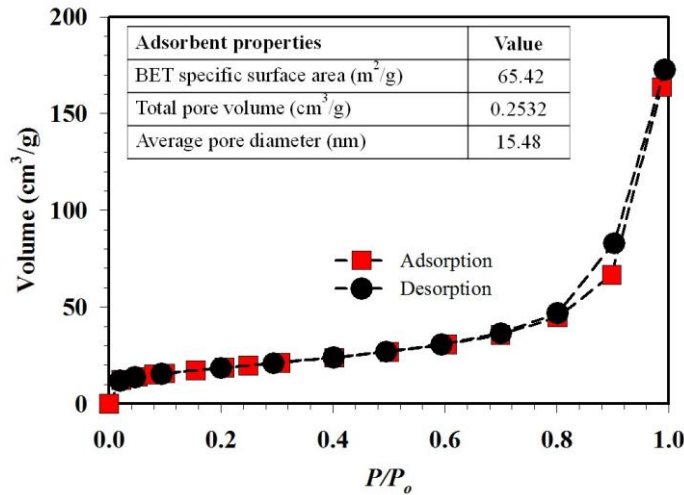


Figure 3. Adsorption-desorption isotherm of N₂ for the IOP adsorbent obtained at 77 K (inset table) Adsorbent properties.

3.2 Effect of the IOP adsorbent dose

The relationship between Cr(VI) adsorption and IOP dose from an aqueous solution was investigated for adsorbent doses ranging from 0.5 to 4.0 g/L. Results revealed (Figure 4) that removal affinity of Cr(VI) was elevated from 11% to 67% and 82% when the IOP doses were increased from 0.5 g/L to 3.0 g/L and 4.0 g/L, respectively. Because total number of available adsorptive sites was related to the amount of IOP dosage, the removal efficiencies of Cr(VI) sharply increased with increasing adsorbent doses (Fang et al., 2011; Rajput et al., 2016). Additionally, a lower removal rate of Cr(VI) at an IOP dosage of below 4.0 g/L implied that the accessible adsorption sites may not be

sufficient to remove Cr(VI) under these experimental conditions. Therefore, an IOP dosage of 4 g/L was suitably selected as an optimum adsorbent dose in the subsequent kinetic adsorption experiments.

The adsorption capacities of Cr(VI) by IOP (Figure 4) ranged from 2.38–2.44 mg/g at the IOP doses between 0.5 g/L and 3.0 g/L and then slightly decreased to 2.21 mg/g at the IOP dose of 4.0 g/L. This suggested a lower utilization of the adsorptive capacity at a high adsorbent dosage, which caused a decrease in Cr(VI) being adsorbed on the adsorptive sites of IOP; this result is consistent with the finding of Ding et al. (2012) who reported that a higher adsorbent dosage exhibited a lower adsorption capacity.

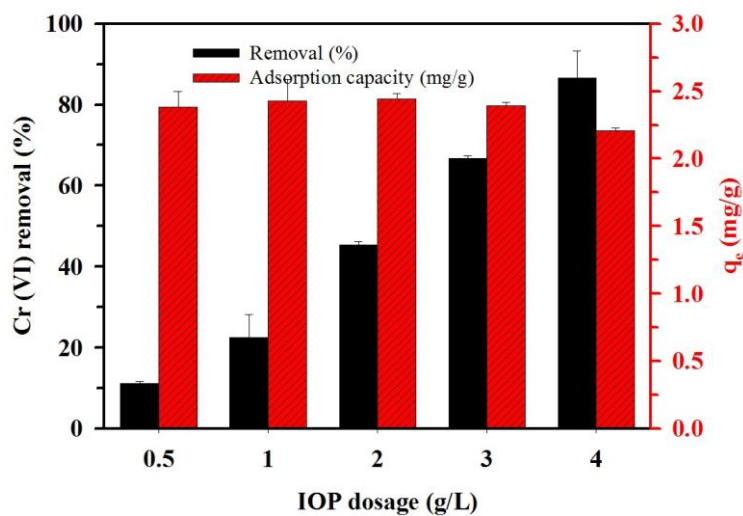


Figure 4. Relationship between Cr(VI) adsorption and IOP dose (Experiment conditions: [Cr(VI)] of 10 mg/L, pH 6.5±0.2, and contact time of 24 h).

3.3 Effect of IOP contact time

The time courses of the Cr(VI) reduction by the IOP is shown in Figure 5. The amounts of Cr(VI) removal elevated with increasing contact times, where removal efficiency of Cr(VI) by the IOPs was initially high, being 60% and 80% after the contact times of 1 and 30 min, respectively, and then slowed down to 86% at the contact time of 120 min. This reflects that larger numbers of adsorptive sites were available for adsorbate during the initial short contact times (Nuhoglu and Malkoc, 2009; Tang et al., 2013; Ding et al., 2012). A small increase in removing of Cr(VI) between the contact times of 30 and 120 min implied that the removal efficiency of

Cr(VI) on IOP reached equilibrium at 30 min. The initial rapid removal rate of Cr(VI) by IOP and the following slower rates were also reported with other adsorbents (Qiu et al., 2014; Liu et al., 2010) and associated with the amorphous structure of the IOP adsorbent. Meanwhile, the reactive adsorption sites of IOP are mostly located on the external surface (Ha et al., 2004), which is different from the interior adsorption by the porous AC (Gupta et al., 2011; Ha et al., 2004). Thus, based on the structure of IOP, Cr(VI) removal by IOP adsorbent can occur rapidly through the surface coordinative reactions of Cr(VI) versus IOP adsorbent.

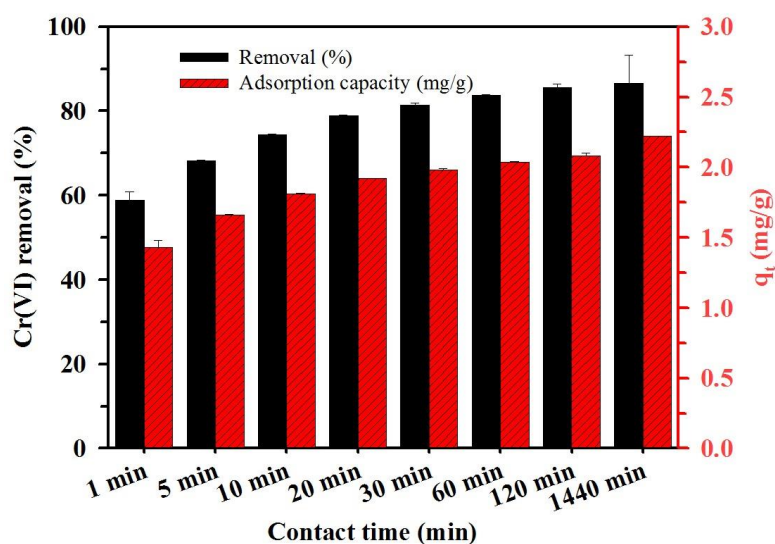


Figure 5. Relationship between Cr(VI) adsorption and contact time (Experiment conditions: [Cr(VI)] of 10 mg/L, pH of 6.5 ± 0.2 , and initial IOP dose of 4 g/L).

3.4 Adsorption isotherm of Cr(VI) by IOPs

The linearized plots of Langmuir and Freundlich isotherm of the equilibrium adsorption of Cr(VI) by IOP is exhibited in Figure 6. The adsorption clearly followed the Langmuir adsorption isotherm model. Hence, the adsorptive behavior of Cr(VI) onto the IOPs is forming a monolayer type, where the Cr(VI) adsorption is restricted by the number and affinity of binding sites on the IOP adsorbent (Langmuir, 1918). The q_{max} of Cr(VI) adsorption by IOP, as calculated from the Langmuir adsorption isotherm model, closely matched that from the experimental data (q_{exp}), further supporting

that the Langmuir adsorption isotherm model was appropriate to describe the Cr(VI) adsorption by IOP. Furthermore, the Langmuir constant of Cr(VI) adsorption by IOP was relatively high, indicating a high affinity of IOP with Cr(VI), which corresponded to the finding of Limcharoensuk et al. (2015). To estimate the potential adsorption probability relationship between solid and liquid, the value of R_L (Limcharoensuk et al., 2015) was calculated (Table 1). Under the conditions used in this study, the calculated R_L value for Cr(VI) adsorption on the IOPs was 0.005, indicating a favorable adsorption.

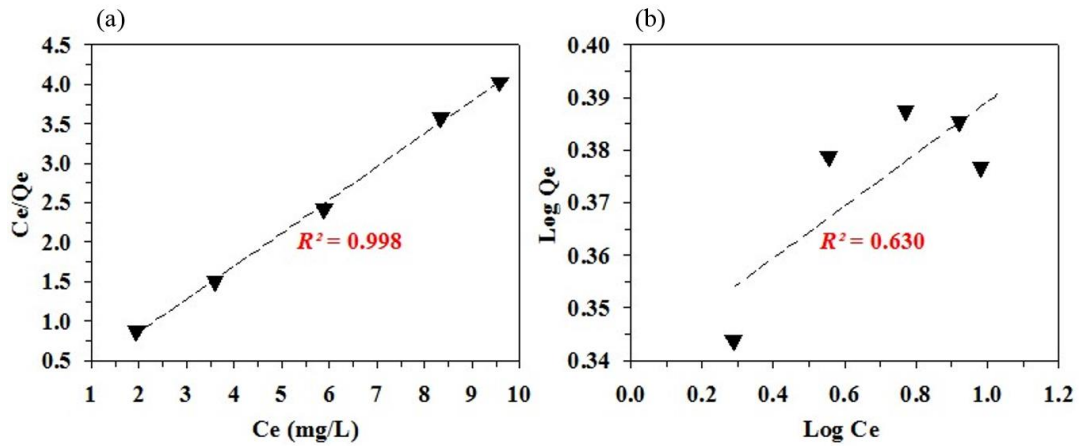


Figure 6. Plot of the equilibrium Cr(VI) adsorption onto IOP for the (a) Langmuir isotherm and (b) Freundlich isotherm models at 25 °C, pH 6.5±0.2. Shown are the linear regression line (dashed) and the corresponding correlation coefficient (R^2) between this and the experimental data (triangles).

Table 1. Cr(VI) adsorption by IOP at pH 6.5±0.2 using Langmuir and Freundlich adsorption isotherm models.

Metal	Langmuir isotherm				Freundlich isotherm		
	q_{max} (mg/g)	b (L/mg)	R^2	R_L	K_f (mg/g)	n	R^2
Cr(VI)	2.39	19.86	0.998	0.005	2.19	20.16	0.630

3.5 Kinetics adsorption of Cr(VI)

The plot of kinetic adsorption of Cr(VI) by IOP for a pseudo-first order model and pseudo-second order model is shown in Figure 7, while kinetic parameters is summarized in Table 2. The data of kinetics adsorption of Cr(VI) on IOP were poorly fitted with the pseudo-first order model, with a relatively low R^2 (0.758) and substantial differences between the theoretical and experimental equilibrium adsorption capacities. The pseudo-

second order model exhibited a good correlation with the kinetic adsorption data with a high R^2 (close to 1.000) and with similar theoretical and experimental equilibrium adsorption capacities (2.10 mg/g and 2.22 mg/g, respectively). Therefore, the Cr(VI) adsorption onto IOP follows the pseudo-second order model, where the rate controlling step is the chemical interaction between the adsorption sites present on the surface of IOP and the Cr(VI) ions (Gupta and Bhattacharya, 2011).

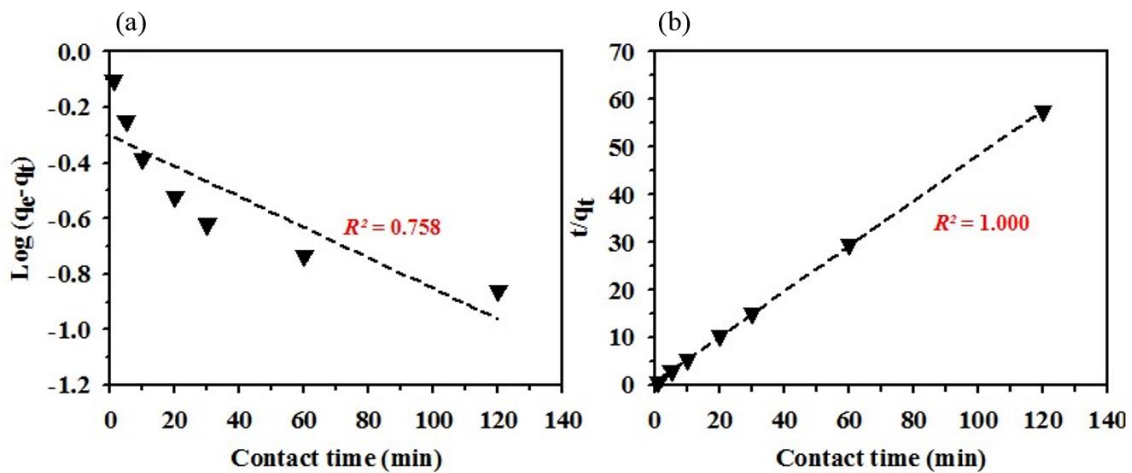


Figure 7. Plot of kinetic adsorption for the (a) pseudo-first-order and (b) pseudo-second-order model of Cr(VI) adsorption by IOP (4 g/L) at 25 °C, pH 6.5±0.2. Shown are the linear regression line (dashed) and the corresponding correlation coefficient (R^2) between this and the experimental data (triangles).

Table 2. Cr(VI) adsorption by IOP at pH 6.5±0.2 using pseudo-first order and pseudo-second order adsorption models.

Metal	q_{exp} (mg/g)	Pseudo-first order kinetic			Pseudo-second order kinetic		
		q_{cal} (mg/g)	k_1 (L/min)	R^2	q_{cal} (mg/g)	k_2 (g/mg.min)	R^2
Cr(VI)	2.22	0.50	0.013	0.758	2.10	0.331	1.000

3.6 Comparison of the q_{max} values of Cr(VI) by various adsorbents

The q_{max} values of Cr(VI) by different adsorbents from the literature reports compared to IOPs (this study) is shown in Table 3. The IOP adsorbent showed a higher q_{max} value of Cr(VI) than some adsorbents reported earlier, such as various AC adsorbents (Hamadi et al., 2001; Choi et al., 2009a; Choi et al., 2009b), but was lower than some other adsorbents (Chaudhuri and Azizan, 2012; Rajput et al., 2016; Qiu et al., 2014; Liu et al., 2010; Ghosh, 2009). The discrepancy of q_{max} values for Cr(VI) among adsorbents could be attributed to the different solutions chemistry and affinities of adsorbent for Cr(VI). For example, competitive anions in aqueous solutions can reduce Cr(VI) adsorption. Overall, the q_{max} of IOP adsorbent for Cr(VI) was in an

appropriate range compared to the other adsorbents. The equilibrium Cr(VI) adsorption for IOP adsorbent was fairly fast (30 min), whereas most of the other adsorbents exhibited very slow adsorption kinetics. Furthermore, the IOP adsorbent can be rapidly separated from the water by installing a magnetic separator in the adsorption process and then collected from the treatment system. Adsorption capacity of Cr(VI) by IOPs after regeneration should be investigated in the future study to explore several efficient and safe methods for the Cr(VI) recovery. However, the Cr(VI) accumulated IOPs can be incinerated and safely disposed in specialized dumps (Habibul et al., 2016). Hence, the IOPs could potentially be a promising adsorbent in removing Cr(VI) from aqueous solutions.

Table 3. Comparison of the q_{max} values of Cr(VI) for the IOP used in this study with those of different adsorbents.

Adsorbent	pH	q_{max} (mg/g)	Reference
Coconut coir AC	1.5-2.0	38.50	Chaudhuri and Azizan (2012)
Magnetite nanoparticles	2.0	20.20	Rajput et al. (2016)
Polyaniline Coated Ethyl Cellulose	1.0	19.49	Qiu et al. (2014)
Fe-modified AC from <i>Trapa natans</i> husk	6.0	11.83	Liu et al. (2010)
Sawdust	2.0	1.90	Hamadi et al. (2001)
Granular AC	–	0.99	Choi et al. (2009a)
AC	–	0.572	Choi et al. (2009b)
Hexadecyltrimethylammonium bromide-modified AC	–	1.82	Choi et al. (2009b)
Cetylpridinium chloride-modified AC	–	1.66	Choi et al. (2009b)
Sulfuric acid-modified waste AC	2.0	7.49	Ghosh (2009)
IOP adsorbent	6.5	2.39	This study

4. CONCLUSIONS

In this study, IOP was synthesized by chemical co-precipitation and found to be an effective adsorbent for Cr(VI) adsorption from aqueous solution. The IOP adsorbent exhibited an efficient Cr(VI) adsorption capacity, with a very fast initial Cr(VI) adsorption rate. The adsorption system followed a Langmuir isotherm, indicating a monolayer adsorption and sorption on a homogenous surface of the IOPs, and was best fitted by pseudo-

second-order model, demonstrating that sorption on the IOPs was by chemisorption. Overall, the IOPs showed a high potential as an effective adsorbent for Cr(VI) removal from aqueous solutions.

ACKNOWLEDGEMENTS

The authors acknowledge the research grant from Kurita Water and Environment Foundation (2016). The authors are grateful to the Coax Group Corporation Co., LTD, Thailand for the SEM

analyses. This study was partially supported by the ICTM grant of the Faculty of Tropical Medicine, Mahidol University.

REFERENCES

- Abussaud B, Ihsanullah HAA, Saleh TA, Gupta VK, Laoui T, Atieh MA. Sorption of phenol from waters on activated carbon impregnated with iron oxide, aluminum oxide and titanium oxide. *Journal of Molecular Liquids* 2013;213:351-9.
- Benito Y, Ruíz ML. Reverse osmosis applied to metal finishing wastewater. *Desalination* 2002;142:229-34.
- Chaudhuri M, Azizan NKB. Adsorptive removal of chromium (VI) from aqueous solution by an agricultural waste-based activated carbon. *Water, Air, and Soil Pollution* 2012;223:1765-71.
- Choi H-D, Cho J-M, Baek K, Yang J-S, Lee J-Y. Influence of cationic surfactant on adsorption of Cr(VI) onto activated carbon. *Journal of Hazardous Materials* 2009a;161:1565-8.
- Choi H-D, Jung W-S, Cho J-M, Ryu B-G, Yang J-S, Baek K. Adsorption of Cr(VI) onto cationic surfactant-modified activated carbon. *Journal of Hazardous Materials* 2009b;166:642-6.
- Deng Y, Qi D, Deng C, Zhang X, Zhao D. Superparamagnetic high-magnetization microspheres with an Fe₃O₄-SiO₂ core and perpendicularly aligned mesoporous SiO₂ shell for removal of microcystins. *Journal of the American Chemical Society* 2008; 130:28-9.
- Ding L, Deng H, Wu C, Han X. Affecting factors, equilibrium, kinetics and thermodynamics of bromide removal from aqueous solutions by MIEX resin. *Chemical Engineering Journal* 2012;181-182:360-70.
- Fang Z, Qiu X, Huang R, Qiu X, Li M. Removal of chromium in electroplating wastewater by nanoscale zero-valent metal with synergistic effect of reduction and immobilization. *Desalination* 2011;280:224-31.
- Faulconer EK, Reitzenstein NVH, Mazyck DW. Optimization of magnetic powdered activated carbon for aqueous Hg(II) removal and magnetic recovery. *Journal of Hazardous Materials* 2012;199-200:9-14.
- Freundlich H. Over the adsorption in solution. *Journal of Physical Chemistry* 1906;57:385-470.
- Ghosh PK. Hexavalent chromium [Cr(VI)] removal by acid modified waste activated carbons. *Journal of Hazardous Materials* 2009;171:116-22.
- Gupta SS, Bhattacharyya KG. Kinetics of adsorption of metal ions on inorganic materials: a review. *Advances in Colloid and Interface Science* 2011;162:39-58.
- Gupta VK, Agarwal S, Saleh TA. Chromium removal by combining the magnetic properties of iron oxide with adsorption properties of carbon nanotubes. *Water Research* 2011;45:2207-12.
- Habibul N, Hu Y, Wang YK, Chen W, Yu H-Q, Sheng G-P. Bioelectrochemical chromium(VI) removal in plant-microbial fuel cells. *Environmental Science and Technology* 2016;50:3882-9.
- Hamadi NK, Chen XD, Farid MM, Lu MGQ. Adsorption kinetics for the removal of chromium(VI) from aqueous solution by adsorbents derived from used tyres and sawdust. *Chemical Engineering Journal* 2001;84:95-105.
- Han Z, Sani B, Mroziak W, Obst M, Beckingham B, Karapanagioti HK, Werner D. Magnetite impregnation effects on the sorbent properties of activated carbons and biochars. *Water Research* 2015;70:394-403.
- Ha TW, Choo KH, Choi S-J. Effect of chlorine on adsorption/ultrafiltration treatment for removing natural organic matter in drinking water. *Journal of Colloid and Interface Science* 2004;274:587-93.
- Ho Y, McKay G, Wase D, Forster C. Study of the sorption of divalent metal ions on to peat. *Adsorption Science and Technology* 2000;18:639-50.
- Hu J, Chen G, Lo IMC. Removal and recovery of Cr(VI) from wastewater by maghemite nanoparticles. *Water Research* 2005;39:4528-36.
- Hu J, Lo IMC, Chen G. Removal of Cr(VI) by magnetite nanoparticle. *Water Science and Technology* 2004; 50:139-46.
- Kongsricharoen N, Polprasert C. Electrochemical precipitation of chromium (Cr⁶⁺) from an electroplating wastewater. *Water Science and Technology* 1995;31:109-17.
- Lagergren S. Zur theorie der sogenannten adsorption gelöster stoffe. *Kungliga Svenska Vetenskapsakademiens Handlingar* 1898;24:1-39.
- Lai KCK, Lo IMC. Removal of Chromium (VI) by Acid-Washed Zero-Valent Iron under Various Groundwater Geochemistry Conditions. *Environmental Science and Technology* 2008;42:1238-44.
- Langmuir I. The adsorption of gases on plane surfaces of glass, mica and platinum. *Journal of the American Chemical Society* 1918;40:1361-403.
- Lei Y, Chen F, Luo Y, Zhang L. Synthesis of three-dimensional graphene oxide foam for the removal of heavy metal ions. *Chemical Physics Letters* 2014; 593:122-7.
- Limcharoensuk T, Sooksawat N, Sumarnrote A, Awutpet T, Kruatrachue M, Pokethitiyook P, Auesukaree C. Bioaccumulation and biosorption of Cd²⁺ and Zn²⁺ by bacteria isolated from a zinc mine in Thailand. *Ecotoxicology and Environmental Safety* 2015; 122:322-30.
- Liu W, Zhang J, Zhang C, Wang Y, Li Y. Adsorptive removal of Cr (VI) by Fe-modified activated carbon prepared from *Trapa natans* husk. *Chemical Engineering Journal* 2010;162:677-84.

- Lu Y, Yin Y, Mayers BT, Xia Y. Modifying the surface properties of superparamagnetic iron oxide nanoparticles through a sol-gel approach. *Nano Letters* 2002;2:183-6.
- Nuhoglu Y, Malkoc E. Thermodynamic and kinetic studies for environmentally friendly Ni(II) biosorption using waste pomace of olive oil factory. *Bioresource Technology* 2009;100:2375-80.
- Oliveira LCA, Rios RVRA, Fabris JD, Garg V, Sapag K, Lago RM. Activated carbon/iron oxide magnetic composites for the adsorption of contaminants in water. *Carbon* 2002;40:2177-83.
- Qiu B, Xu C, Sun D, Yi H, Guo J, Zhang X, Qu H, Guerrero M, Wang X, Noel N, Luo Z, Guo Z, Wei S. Polyaniline coated ethyl cellulose with improved hexavalent chromium removal. *ACS Sustainable Chemistry and Engineering* 2014;2:2070-80.
- Rajput S, Pittman CU, Mohan D. Magnetic magnetite (Fe_3O_4) nanoparticle synthesis and applications for lead (Pb^{2+}) and chromium (Cr^{6+}) removal from water. *Journal of Colloid and Interface Science* 2016; 468:334-46.
- Rengaraj S, Yeon K-H, Moon S-H. Removal of chromium from water and wastewater by ion exchange resins. *Journal of Hazardous Materials* 2001;87:273-87.
- Sing K. Reporting physisorption data for gas/solid systems with special reference to the determination of surface area and porosity (Provisional). *Pure and Applied Chemistry* 1982;54:2201-18.
- Suksabye P, Thiravetyan P, Nakbanpote W. Column study of chromium (VI) adsorption from electroplating industry by coconut coir pith. *Journal of Hazardous Materials* 2008;160:56-62.
- Tang Y, Liang S, Guo H, You H, Gao N, Yu S. Adsorptive characteristics of perchlorate from aqueous solutions by MIEX resin. *Colloids and Surfaces A: Physicochemical and Engineering Aspects* 2013; 417:26-31.
- Uwamariya V, Petrusevski B, Slokar YM, Aubry C, Lens PNL, Amy GL. Effect of fulvic acid on adsorptive removal of Cr(VI) and As(V) from groundwater by iron oxide-based adsorbents. *Water, Air, and Soil Pollution* 2015;226:1-12.
- Zou Z, Tang Y, Jiang C, Zhang J. Efficient adsorption of Cr(VI) on sunflower seed hull derived porous carbon. *Journal of Environmental Chemical Engineering* 2015;3:898-905.